Biomedical Optics EXPRESS

Dynamic functional connectivity revealed by resting-state functional near-infrared spectroscopy

Zhen Li,[1,2] Hanli Liu,[3] Xuhong Liao,[1,2] Jingping Xu,[1,2] Wenli Liu,[1,2] Fenghua Tian,[3] Yong He,[1,2] Haijing Niu[1,2,*]

[1]*State Key Laboratory of Cognitive Neuroscience and Learning & IDG/McGovern Institute for Brain Research, Beijing Normal University, Beijing, 100875 China*

[2]*Center for Collaboration and Innovation in Brain and Learning Sciences, Beijing Normal University, Beijing, 100875 China*

[3] *Department of Bioengineering, the University of Texas at Arlington, Arlington, Texas, USA*

**niuhjing@bnu.edu.cn*

Abstract: The brain is a complex network with time-varying functional connectivity (FC) and network organization. However, it remains largely unknown whether resting-state fNIRS measurements can be used to characterize dynamic characteristics of intrinsic brain organization. In this study, for the first time, we used the whole-cortical fNIRS time series and a sliding-window correlation approach to demonstrate that fNIRS measurement can be ultimately used to quantify the dynamic characteristics of resting-state brain connectivity. Our results reveal that the fNIRS-derived FC is time-varying, and the variability strength (Q) is correlated negatively with the time-averaged, static FC. Furthermore, the Q values also show significant differences in connectivity between different spatial locations (e.g., intrahemispheric and homotopic connections). The findings are reproducible across both sliding-window lengths and different brain scanning sessions, suggesting that the dynamic characteristics in fNIRS-derived cerebral functional correlation results from true cerebral fluctuation.

OCIS codes: (170.2655) Functional monitoring and imaging; (170.5380) Physiology; (170.3880) Medical and biological imaging.

References and links

1. O. Sporns and J. D. Zwi, "The small world of the cerebral cortex," Neuroinformatics **2**(2), 145–162 (2004).
2. E. A. Allen, E. Damaraju, S. M. Plis, E. B. Erhardt, T. Eichele, and V. D. Calhoun, "Tracking whole-brain connectivity dynamics in the resting state," Cereb. Cortex **24**(3), 663–676 (2014).
3. C. Chang and G. H. Glover, "Time-frequency dynamics of resting-state brain connectivity measured with fMRI," Neuroimage **50**(1), 81–98 (2010).
4. C. J. Chu, M. A. Kramer, J. Pathmanathan, M. T. Bianchi, M. B. Westover, L. Wizon, and S. S. Cash, "Emergence of stable functional networks in long-term human electroencephalography," J. Neurosci. **32**(8), 2703–2713 (2012).
5. F. de Pasquale, S. Della Penna, A. Z. Snyder, C. Lewis, D. Mantini, L. Marzetti, P. Belardinelli, L. Ciancetta, V. Pizzella, G. L. Romani, and M. Corbetta, "Temporal dynamics of spontaneous MEG activity in brain networks," Proc. Natl. Acad. Sci. U.S.A. **107**(13), 6040–6045 (2010).
6. R. M. Hutchison, T. Womelsdorf, E. A. Allen, P. A. Bandettini, V. D. Calhoun, M. Corbetta, S. Della Penna, J. H. Duyn, G. H. Glover, J. Gonzalez-Castillo, D. A. Handwerker, S. Keilholz, V. Kiviniemi, D. A. Leopold, F. de Pasquale, O. Sporns, M. Walter, and C. Chang, "Dynamic functional connectivity: promise, issues, and interpretations," Neuroimage **80**, 360–378 (2013).
7. R. M. Hutchison, T. Womelsdorf, J. S. Gati, S. Everling, and R. S. Menon, "Resting-state networks show dynamic functional connectivity in awake humans and anesthetized macaques," Hum. Brain Mapp. **34**(9), 2154–2177 (2013).
8. M. A. Kramer, U. T. Eden, K. Q. Lepage, E. D. Kolaczyk, M. T. Bianchi, and S. S. Cash, "Emergence of persistent networks in long-term intracranial EEG recordings," J. Neurosci. **31**(44), 15757–15767 (2011).

#237175 - $15.00 USD Received 30 Mar 2015; revised 27 May 2015; accepted 28 May 2015; published 5 Jun 2015

9. A. Zalesky, A. Fornito, L. Cocchi, L. L. Gollo, and M. Breakspear, "Time-resolved resting-state brain networks," Proc. Natl. Acad. Sci. USA **111**(28), 10341–10346 (2014).
10. E. Damaraju, J. Turner, A. Preda, T. Van Erp, D. Mathalon, J. M. Ford, S. Potkin, and V. D. Calhoun, "Static and dynamic functional network connectivity during resting state in schizophrenia," American College of Neuropsychopharmacology, Hollywood, CA (2012).
11. P. E. Holtzheimer and H. S. Mayberg, "Stuck in a rut: rethinking depression and its treatment," Trends Neurosci. **34**(1), 1–9 (2011).
12. D. T. Jones, P. Vemuri, M. C. Murphy, J. L. Gunter, M. L. Senjem, M. M. Machulda, S. A. Przybelski, B. E. Gregg, K. Kantarci, D. S. Knopman, B. F. Boeve, R. C. Petersen, and C. R. Jack, Jr., "Non-stationarity in the "resting brain's" modular architecture," PLoS ONE **7**(6), e39731 (2012).
13. D. A. Boas, A. M. Dale, and M. A. Franceschini, "Diffuse optical imaging of brain activation: approaches to optimizing image sensitivity, resolution, and accuracy," Neuroimage **23**(Suppl 1), S275–S288 (2004).
14. H. Niu and Y. He, "Resting-state functional brain connectivity: lessons from functional near-infrared spectroscopy," Neuroscientist **20**(2), 173–188 (2014).
15. A. Villringer and B. Chance, "Non-invasive optical spectroscopy and imaging of human brain function," Trends Neurosci. **20**(10), 435–442 (1997).
16. B. R. White, A. Z. Snyder, A. L. Cohen, S. E. Petersen, M. E. Raichle, B. L. Schlaggar, and J. P. Culver, "Resting-state functional connectivity in the human brain revealed with diffuse optical tomography," Neuroimage **47**(1), 148–156 (2009).
17. H. Zhang, Y. J. Zhang, C. M. Lu, S. Y. Ma, Y. F. Zang, and C. Z. Zhu, "Functional connectivity as revealed by independent component analysis of resting-state fNIRS measurements," Neuroimage **51**(3), 1150–1161 (2010).
18. C. M. Lu, Y. J. Zhang, B. B. Biswal, Y. F. Zang, D. L. Peng, and C. Z. Zhu, "Use of fNIRS to assess resting state functional connectivity," J. Neurosci. Methods **186**(2), 242–249 (2010).
19. Y. J. Zhang, C. M. Lu, B. B. Biswal, Y. F. Zang, D. L. Peng, and C. Z. Zhu, "Detecting resting-state functional connectivity in the language system using functional near-infrared spectroscopy," J. Biomed. Opt. **15**(4), 047003 (2010).
20. H. Niu, Z. Li, X. Liao, J. Wang, T. Zhao, N. Shu, X. Zhao, and Y. He, "Test-retest reliability of graph metrics in functional brain networks: a resting-state fNIRS study," PLoS ONE **8**(9), e72425 (2013).
21. H. Zhang, L. Duan, Y. J. Zhang, C. M. Lu, H. Liu, and C. Z. Zhu, "Test-retest assessment of independent component analysis-derived resting-state functional connectivity based on functional near-infrared spectroscopy," Neuroimage **55**(2), 607–615 (2011).
22. F. Homae, H. Watanabe, T. Otobe, T. Nakano, T. Go, Y. Konishi, and G. Taga, "Development of global cortical networks in early infancy," J. Neurosci. **30**(14), 4877–4882 (2010).
23. B. R. White, S. M. Liao, S. L. Ferradal, T. E. Inder, and J. P. Culver, "Bedside optical imaging of occipital resting-state functional connectivity in neonates," Neuroimage **59**(3), 2529–2538 (2012).
24. J. A. Turner, E. Damaraju, T. G. van Erp, D. H. Mathalon, J. M. Ford, J. Voyvodic, B. A. Mueller, A. Belger, J. Bustillo, S. McEwen, S. G. Potkin, Fbirn, and V. D. Calhoun, "A multi-site resting state fMRI study on the amplitude of low frequency fluctuations in schizophrenia," Front. Neurosci. **7**, 137 (2013).
25. P. Delamillieure, G. Doucet, B. Mazoyer, M. R. Turbelin, N. Delcroix, E. Mellet, L. Zago, F. Crivello, L. Petit, N. Tzourio-Mazoyer, and M. Joliot, "The resting state questionnaire: An introspective questionnaire for evaluation of inner experience during the conscious resting state," Brain Res. Bull. **81**(6), 565–573 (2010).
26. S. Kohno, I. Miyai, A. Seiyama, I. Oda, A. Ishikawa, S. Tsuneishi, T. Amita, and K. Shimizu, "Removal of the skin blood flow artifact in functional near-infrared spectroscopic imaging data through independent component analysis," J. Biomed. Opt. **12**(6), 062111 (2007).
27. B. Biswal, F. Z. Yetkin, V. M. Haughton, and J. S. Hyde, "Functional connectivity in the motor cortex of resting human brain using echo-planar mri," Magn. Reson. Med. **34**(4), 537–541 (1995).
28. D. A. Handwerker, V. Roopchansingh, J. Gonzalez-Castillo, and P. A. Bandettini, "Periodic changes in fMRI connectivity," Neuroimage **63**(3), 1712–1719 (2012).
29. V. Kiviniemi, T. Vire, J. Remes, A. A. Elseoud, T. Starck, O. Tervonen, and J. Nikkinen, "A sliding time-window ICA reveals spatial variability of the default mode network in time," Brain Connect **1**(4), 339–347 (2011).
30. U. Sakoğlu, G. D. Pearlson, K. A. Kiehl, Y. M. Wang, A. M. Michael, and V. D. Calhoun, "A method for evaluating dynamic functional network connectivity and task-modulation: application to schizophrenia," MAGMA **23**(5-6), 351–366 (2010).
31. D. S. Bassett, N. F. Wymbs, M. A. Porter, P. J. Mucha, J. M. Carlson, and S. T. Grafton, "Dynamic reconfiguration of human brain networks during learning," Proc. Natl. Acad. Sci. U.S.A. **108**(18), 7641–7646 (2011).
32. N. A. Crossley, A. Mechelli, P. E. Vértes, T. T. Winton-Brown, A. X. Patel, C. E. Ginestet, P. McGuire, and E. T. Bullmore, "Cognitive relevance of the community structure of the human brain functional coactivation network," Proc. Natl. Acad. Sci. U.S.A. **110**(28), 11583–11588 (2013).
33. T. H. Bullock, "Have brain dynamics evolved? Should we look for unique dynamics in the sapient species?" Neural Comput. **15**(9), 2013–2027 (2003).
34. D. L. Ringach, "Spontaneous and driven cortical activity: implications for computation," Curr. Opin. Neurobiol. **19**(4), 439–444 (2009).

#237175 - $15.00 USD Received 30 Mar 2015; revised 27 May 2015; accepted 28 May 2015; published 5 Jun 2015

35. S. Sadaghiani, G. Hesselmann, K. J. Friston, and A. Kleinschmidt, "The relation of ongoing brain activity, evoked neural responses, and cognition," Front. Syst. Neurosci. **4**, 20 (2010).
36. T. P. Vogels, K. Rajan, and L. F. Abbott, "Neural network dynamics," Annu. Rev. Neurosci. **28**(1), 357–376 (2005).
37. M. W. Cole, A. Bagic, R. Kass, and W. Schneider, "Prefrontal dynamics underlying rapid instructed task learning reverse with practice," J. Neurosci. **30**(42), 14245–14254 (2010).
38. H. Niu, J. Wang, T. Zhao, N. Shu, and Y. He, "Revealing topological organization of human brain functional networks with resting-state functional near infrared spectroscopy," PLoS ONE **7**(9), e45771 (2012).
39. A. M. Hermundstad, D. S. Bassett, K. S. Brown, E. M. Aminoff, D. Clewett, S. Freeman, A. Frithsen, A. Johnson, C. M. Tipper, M. B. Miller, S. T. Grafton, and J. M. Carlson, "Structural foundations of resting-state and task-based functional connectivity in the human brain," Proc. Natl. Acad. Sci. USA **110**(15), 6169–6174 (2013).
40. S. W. Davis, J. E. Kragel, D. J. Madden, and R. Cabeza, "The Architecture of Cross-Hemispheric Communication in the Aging Brain: Linking Behavior to Functional and Structural Connectivity," Cereb. Cortex **22**(1), 232–242 (2012).
41. D. E. Stark, D. S. Margulies, Z. E. Shehzad, P. Reiss, A. M. Kelly, L. Q. Uddin, D. G. Gee, A. K. Roy, M. T. Banich, F. X. Castellanos, and M. P. Milham, "Regional Variation in Interhemispheric Coordination of Intrinsic Hemodynamic Fluctuations," J. Neurosci. **28**(51), 13754–13764 (2008).
42. M.-M. Mesulam, "From sensation to cognition," Brain **121**(6), 1013–1052 (1998).
43. M. D. Greicius, K. Supekar, V. Menon, and R. F. Dougherty, "Resting-state functional connectivity reflects structural connectivity in the default mode network," Cereb. Cortex **19**(1), 72–78 (2009).
44. M. P. van den Heuvel, R. C. W. Mandl, R. S. Kahn, and H. E. Hulshoff Pol, "Functionally linked resting-state networks reflect the underlying structural connectivity architecture of the human brain," Hum. Brain Mapp. **30**(10), 3127–3141 (2009).
45. M. Nasiriavanaki, J. Xia, H. Wan, A. Q. Bauer, J. P. Culver, and L. V. Wang, "High-resolution photoacoustic tomography of resting-state functional connectivity in the mouse brain," Proc. Natl. Acad. Sci. U.S.A. **111**(1), 21–26 (2014).

1. Introduction

The human brain is a dynamic and highly complex network with the capability of generating and integrating information from various sources in real time [1]. Recently, a large number of studies have demonstrated the dynamic fluctuation of the brain in functional connectivity (FC) by monitoring brain activity at rest using functional magnetic resonance imaging (fMRI), electroencephalography (EEG), or magnetoencephalography (MEG) techniques [2–9]. The temporal fluctuations of FC have been shown to be an essential property that is necessary for normal brain function and their disruption is evidence of abnormal brain activity in schizophrenia [10], depression [11], and Alzheimer's disease [12].

The brain imaging technique of functional near-infrared spectroscopy (fNIRS) is an emerging optical tool used to measure functional brain connectivity. The biophysical origin of the technique is the variation in concentrations of oxyhemoglobin (HbO) and deoxyhemoglobin (HbR) in the cerebral cortex that frequently results from changes in cerebral blood flow and the cerebral metabolic rate of oxygen [13–15]. Recent studies have proven the detectability of resting-state FC by fNIRS [14], which characterizes the synchronization of spontaneous neural activities between spatially remote brain regions, such as between bilateral sensorimotor cortices [16, 17], auditory cortices [18], visual cortices [16, 17], and language-related cortices [19]. Such FC measured by fNIRS shows remarkable consistency across adult subjects [20, 21]; however, substantial variations are also seen throughout normal development [22] and during activities indicating neurological disorders [23] in young infants. These accumulated findings indicate the potential value of fNIRS as a useful brain-imaging tool to study functional brain network in varying participant populations.

Currently, the analysis of fNIRS-based resting-state FC typically employs approaches such as seed correlation and independent component analysis [24]. The seed correlation approach utilizes a single correlation coefficient calculated from a pair of time series of the entire temporal scan to represent the relationship between the selected seed(s) and other brain regions of interest [25] over the duration of the temporal scan. Similarly, ICA uses time series over the entire measurement period to identify the spatially independent functional sub-

#237175 - $15.00 USD Received 30 Mar 2015; revised 27 May 2015; accepted 28 May 2015; published 5 Jun 2015

networks. In general, both approaches assume that the strength of interaction between two brain regions is constant or static throughout the duration of the measurement period. However, recent research on dynamic FC has provided compelling evidence that compared to the time-averaged, static resting-state FC, dynamic FC may better reflect and reveal "changes in macroscopic neural activity patterns underlying critical aspects of cognition and behavior" [6, 9]. Thus, studying the dynamic functional brain connectivity is of great importance and advantage that can provide us with an imaging tool to better understand the mechanisms that underlie the dynamic features of the brain. Since the research on dynamic FC is relatively new, there exist limitations regarding data analysis and result interpretation [6, 9]; much research and development in this area are needed. Because fNIRS has a much higher sampling rate than the widely used fMRI technique, fNIRS provides rich temporal information that can be used to investigate the time-varying functional organization in the human brain. Therefore, fNIRS is an excellent research tool to be explored and then used for studying dynamic FC.

The novelty of the present study is to investigate whether and how fNIRS measurements can be ultimately used to quantify the dynamic characteristics of resting-state FC. In the study, a sliding-window correlation (SWC) analysis [6, 9] was performed on fNIRS time series to obtain dynamic network organization at resting state from 18 participants. For data analysis and result interpretation, this study is organized as follows: First, we will demonstrate the characteristics of temporal variation in the resulting FC time series from all participants. Next, we will define and quantify the FC variability strength (Q) and explore the dynamic relationship between FC variability strength Q and static connectivity strength. Subsequently, we will reveal the differences in FC variability across different spatial locations (homotopic, heterotopic, long and short intrahemispheric connections). Finally, we will examine the repeatability of our dynamic FC findings using different window lengths and two separate fNIRS test data sets (Session 1 versus Session 2). The present work, for the first time, utilizes whole-cortical fNIRS time series to derive dynamic FC in the human brain and reveals the fNIRS-based temporal-spatial features of dynamic FC network in the resting-state brain.

2. Materials and methods

2.1 Participants

The data used in this study were obtained from a previous experiment that examined the test-retest reliability of the graph metrics of the resting state fNIRS brain network [20]. Specifically, 21 healthy right-handed college students (17 males and 4 females, ages 21 to 27 years) were recruited and written informed consent was obtained from all participants prior to the experiment. This study was approved by the Institutional Review Board of Beijing Normal University Imaging Center for Brain Research.

2.2 Experimental protocol

This experiment consisted of two sessions of resting-state fNIRS recordings. Each session lasted 11 minutes with intervals between them of approximately 20 minutes. During the recordings, participants were instructed to remain still and keep their eyes closed without falling asleep. During the 20-min interval of the two scanning sessions, participants were instructed to sit (wearing the probe holder) and were allowed slight body and head motion. In the present study, we used the first-session data to perform dynamic FC analysis and then validated our findings with the second-session data.

2.3 Data acquisition

A continuous-wave (CW) near-infrared optical imaging system (CW6, TechEn Inc., MA, USA) was used to measure the variations of the HbO and HbR concentration (Fig. 1(A)). The

#237175 - $15.00 USD Received 30 Mar 2015; revised 27 May 2015; accepted 28 May 2015; published 5 Jun 2015

system generated two wavelengths (690 and 830 nm) of near-infrared light and collected the hemoglobin-dependent signals at a sampling rate of 25 Hz. Twelve light sources (each with two wavelengths) and 24 detectors were designed to conFig. 46-measurement channels to allow for the whole brain (i.e., frontal, temporal, parietal, and occipital lobes) to be covered bilaterally (Fig. 1(B)). The spatial separation between any adjacent source and detector pair was 3.2 cm. The positioning of the probes was set according to the international 10-20 system.

2.4 Data preprocessing

For the time course of HbO or HbR signals, we first conducted a temporal ICA analysis to remove typical motion-induced artifacts and systematic physiological noise [17, 20, 26]. Then, we filtered the data using a band pass filter with a band-pass frequency of 0.01 to 0.1 Hz to reduce the effect of high-frequency noise and baseline drift and, at the same time, we sought to obtain low frequency hemodynamic signals that are thought to emanate from spontaneous neural activity [16, 27]. Finally, we extracted 10-min data from the continuous time course of each participant to conduct dynamic FC analysis. Three of the subjects were excluded due to poor optical contact between the head probe and scalp on at least one measurement channel. The data of the remaining 18 subjects was used for further dynamic FC analysis.

2.5 Dynamic FC calculation and analysis

For each individual data set, we first of all calculated the static FC (Fig. 1(C)) with Pearson correlation analysis between any two time series of the measurement channels. Subsequently, we also calculated the dynamic FC of the signals with a SWC approach (Fig. 1(D)). The SWC is the most commonly used strategy for examining FC dynamics in the present neuroimaging studies [2, 3, 7, 12, 28–30]. In our framework of SWC analysis, a 60-s time window was selected and then shifted in an increment of 1 s along the entire time course. The FC within each time window was quantitatively calculated for each selected pair of brain regions using the Pearson correlation strategy. The 10-min measurement duration and a 60-s time window yielded 541 sliding-time windows and thus resulted in 541 dynamic FC maps.

To demonstrate whether the obtained FC maps at different time windows dynamically fluctuate over time, we had to quantitatively compare them with a common reference map that was chosen to be the static FC map obtained over the entire 10-min time window. Mathematically, each FC correlation map included $46 \times 45/2$ correlation coefficients calculated from any two-measurement channels and could be arranged as a column vector. We formed a total of 541 dynamic FC correlation vectors and one static FC vector. To quantify the similarity between each dynamic FC map with the static FC map, we calculated another correlation coefficient between each dynamic vector and the static vector for each subject. To be clear, we named this new correlation coefficient as "between-map" correlation coefficient, r_m, which was used to quantify the degree of similarity between two maps and the degree of fluctuation between the dynamic FC maps. In this way, each dynamic FC correlation map gave rise to a single r_m with respect to the static FC map. For the entire 10-min window, we obtained a time series of 541 values of r_m for each subject (Fig. 2(B)).

To quantitatively estimate the variability of whole-cortex FC across a series of sliding time windows, we further calculated the spectrum power of the dynamic FC time series (with Fourier analysis) [2]for each participant (see Fig. 7 in appendix). Thus, the area under the curve of the power spectrum across the low frequency (< 0.1 Hz) band was used as a fluctuation strength index, Q, to mark time-varying characteristics of dynamic FC (Fig. 3(A)). A higher Q value represented a more variable FC, whereas a smaller Q value represented a less variable FC. To explore the potential fluctuation properties of dynamic FC, we examined the linear relationship between FC variability strength and the corresponding static

#237175 - $15.00 USD Received 30 Mar 2015; revised 27 May 2015; accepted 28 May 2015; published 5 Jun 2015

connectivity strength using a Spearman correlation analysis at both group and individual levels, respectively.

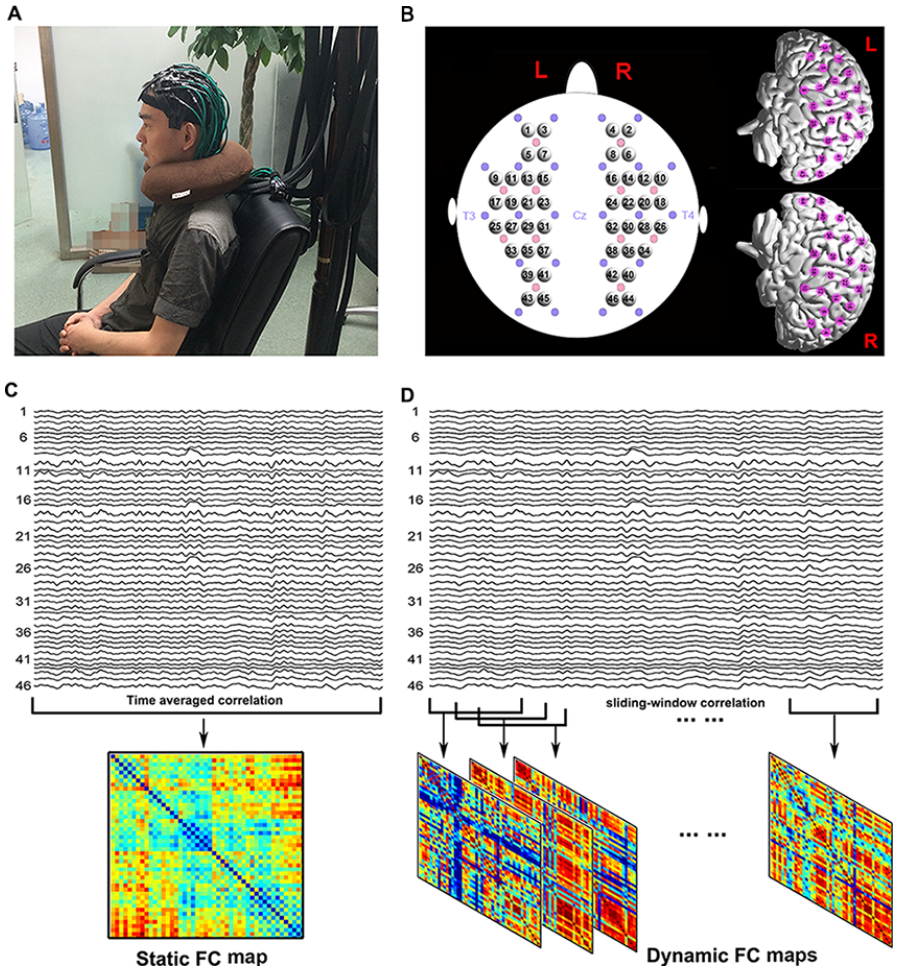

Fig. 1. Illustration of fNIRS-based FC analysis. (A)Photograph of whole-head fNIRS data acquisition on a participant. (B) The schematic of whole-head imaging pad (12 sources, red, and 24 detectors, blue). The sources and detectors were symmetrically placed on the left and right hemispheres and constituted 46 measurement channels, which allowed for the whole brain (i.e., frontal, temporal, parietal, and occipital lobes to be measured. (C) Static FC analysis. The static FC was calculated from time series of entire scanning between any two channels. (D) Dynamic FC analysis. The dynamic FC was calculated using sliding-window correlation approach. In this approach, a time window of fixed length was selected, and data points within that window were used to calculate the FC. The window was then shifted in time by a fixed number of data points. This process results in quantification of the time-varying FC over the duration of the scan.

Furthermore, to reveal whether the values of index Q are different across varying cortical locations, we further classified the entire cortical FC into four spatially different connectivity groups (Fig. 4(A)) and then examined their difference in FC variability strength between groups. These four connectivity groups included: (1) homotopic connectivity, which indicated connectivity between inter-hemispheric homologous regions [23 pairs, i.e., 46/2]; (2) long intrahemispheric connectivity, which indicated connectivity between different anatomical areas in the same hemisphere with a length larger than 10 cm [82 pairs]; (3) short intrahemispheric connectivity, which indicated connectivity between different anatomical

#237175 - $15.00 USD Received 30 Mar 2015; revised 27 May 2015; accepted 28 May 2015; published 5 Jun 2015

areas in the same hemisphere with a length smaller than 10 cm [424 pairs]; and (4) heterotopic connectivity, which indicated connectivity between different anatomical areas in opposite hemispheres [506 pairs].

The statistical analysis of index Q between connectivity groups was performed using permutation testing [31, 32]. First, for each individual connection, the value of index Q was averaged across subjects and then was used as factors for statistical analysis. Second, the between-group differences of the averaged Q values were tested between any two connectivity groups using permutation test. Third, during the permutation test, two random surrogate groups were first generated by randomly assigning each edge (i.e., connectivity) to one of these two groups, while maintaining the same number of edges as the original two groups. Next, the difference in variability index Q between these two random groups was computed. This procedure was repeated for 10,000 permutations, resulting in a sampled between-group difference and null distribution for the index Q. Finally, the observed between-group difference was assigned a p value by counting the proportion of the total number of 10,000 entries resulting from the permutation that was greater than (or smaller than if the effect was negative) the original group difference. A significance threshold of $p < 0.01$ (Bonferroni corrected) was used to confirm the difference in index Q between connectivity groups.

Finally, to assess the effect of time window lengths on dynamic characteristics of FC, we selected two additional window lengths, namely 30 s and 90 s, to repeat the above analysis. Meanwhile, to examine the reproducibility of the dynamic FC findings across scanning sessions, we also adopted a separate fNIRS data set (Session 2) to conduct the same data analysis based on the 60-s sliding-window length.

3. Results

3.1 FC dynamics

As described in Section 2.5, a correlation coefficient map was generated to reflect FC between each pair of channels at different cortical locations. As seen in Figs. 1(C) and 1(D), it is expected that different FC strengths among different channels should give rise to different color patterns. The redder the map pattern is, the stronger the FC is. In a quantitative expression, the value of between-map coefficient, r_m, is close to 1 if the color patterns of two FC maps are similar or close to one another. Otherwise, mismatched color patterns among different FC maps indicate low values of r_m and a relatively large fluctuation among dynamic FC strengths.

Figure 2(A) shows an example of a single participant's 135 dynamic FC maps derived from HbO (left) and HbR (right) signals at a temporal interval of 4 seconds. Visually, while each dynamic map was too small to show details, the overall color patterns and their variability across 135 maps at different time windows might be clearly observed. It was seen that FC patterns between most of time windows displayed noticeable dynamic variations over the 10-min scanning duration. Quantitatively, Fig. 2(B) plots the Pearson "between-map" correlation coefficients, r_m, calculated between the successive dynamic FC maps and the static FC map from Subject 14. This figure displayed strong and notable fluctuations with a mean value and standard deviation of 0.62 ± 0.11 for HbO and 0.76 ± 0.07 for HbR over the scanning duration. Using the same analysis framework, we calculated the temporal fluctuations of FC maps from all 18 participants; all respective values of r_m were temporally mapped in Fig. 2(C). We found that FC of each participant dynamically changed across the duration of scanning, irrespective of HbO and HbR signals, which reflect the expected dynamic neural activities from each participant.

#237175 - $15.00 USD Received 30 Mar 2015; revised 27 May 2015; accepted 28 May 2015; published 5 Jun 2015

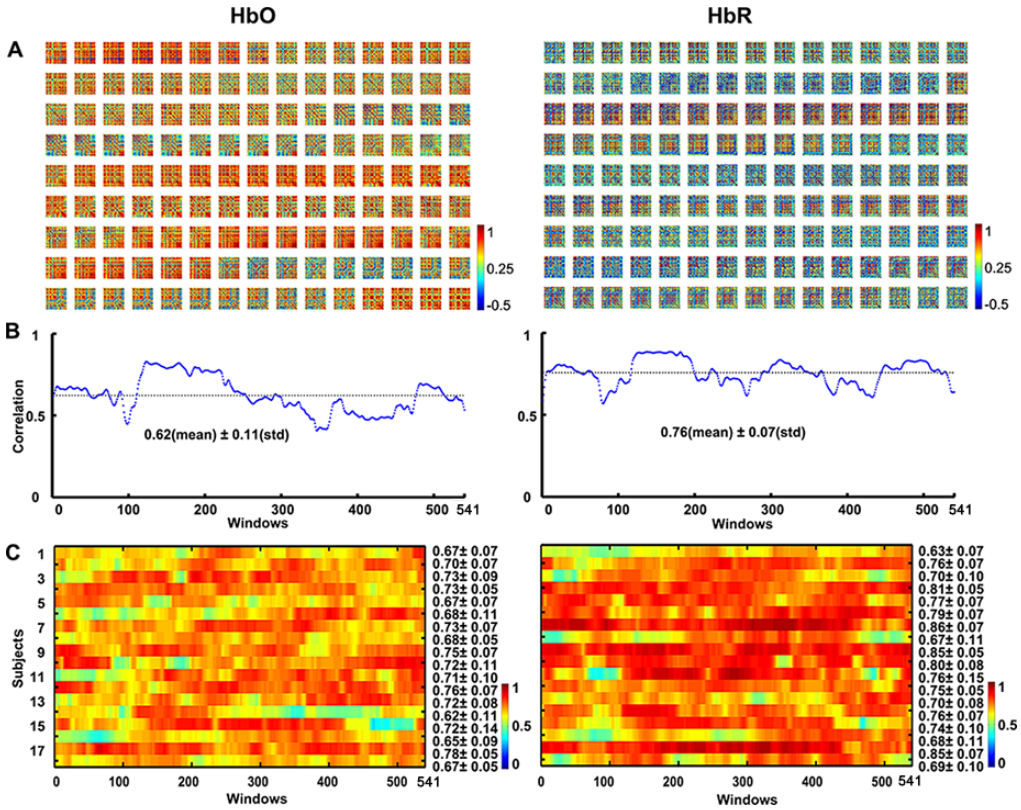

Fig. 2. FC dynamics derived from HbO (left) and HbR (right) signals. (A) An example of dynamic FC maps displayed at an interval of 4 s on an arbitrary participant (Subject 14). (B) The Pearson "between-map" correlation coefficients, r_m, calculated between the successive dynamic FC maps and the static FC map from Subject 14. The dotted straight line represents the mean and standard derivation of r_m across the 10-min time window. (C) Similar calculation to (B) on all 18 subjects. The sliding-window length used to evaluate dynamic FC was 60 s.

3.2 Relationship between FC variability strength and static connectivity strength

Figure 3 shows the group-level FC variability strength (Q), static FC strength as well as the linear relationship between them derived from both HbO and HbR signals, respectively. Visually, the spatial patterns between index Q and the static connectivity strength exhibited a contrary trend. For example, near diagonal connectivity trace of the matrix maps (Figs. 3(A) and 3(B)), a smaller Q value (Fig. 3(A)) was accompanied by a larger static FC strength (Fig. 3(B)). The quantitative correlation analysis between them also revealed that there was a strong and significant negative correlation relationship across both HbO ($r = -0.78$, $p < 10^{-10}$) and HbR ($r = -0.37$, $p < 10^{-10}$) (Fig. 3(C)). The result indicates that the weaker the static connectivity strength, the larger the value of index Q in a series of temporal brain activities and vice-versa. Similarly, the individual-level correlation analysis revealed that the index Q also showed a significantly negative correlation ($p < 0.001$) with the static connectivity strength, which was almost present in all participants across two hemoglobin signals (except for one subject in the HbR signal) (see Table 1 in appendix). The average correlation between index Q and the static connectivity strength across subjects was -0.72 ± 0.16 for HbO and -0.35 ± 0.23 for HbR. Furthermore, the Q values in Fig. 3(A) also illustrated regional differences of FC variability strength in the entire cortical connectivity network. For example, much bigger Q values were found in connectivity between frontal and parietal/occipital cortical regions (Fig. 3(A)).

#237175 - $15.00 USD Received 30 Mar 2015; revised 27 May 2015; accepted 28 May 2015; published 5 Jun 2015

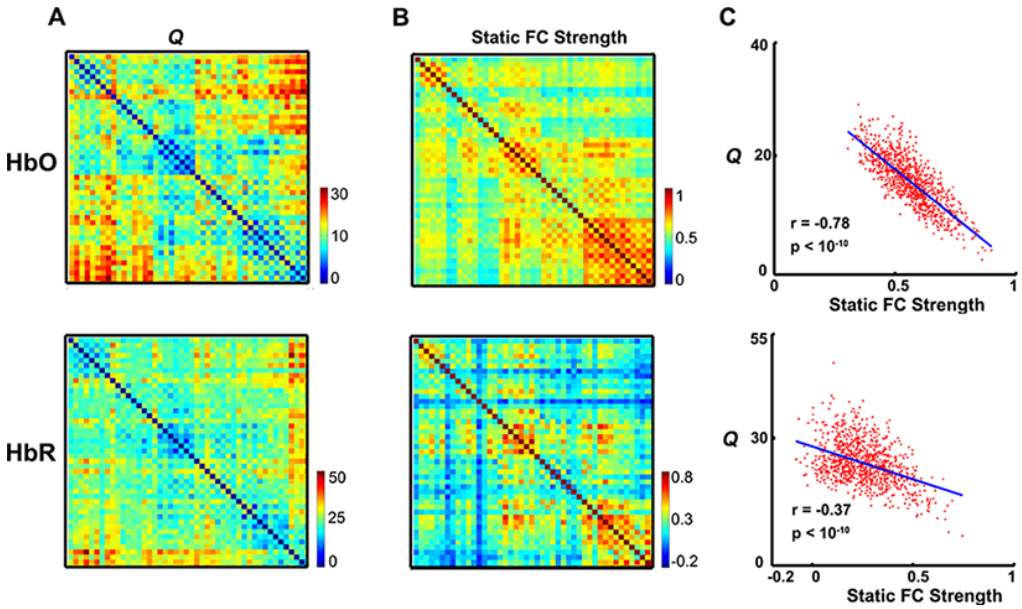

Fig. 3. Pattern comparison between FC variability strength, *Q*, and static FC strength. (A)The group-averaged *Q* values, (B) static FC strength and (C) the linear relationship between them derived from HbO and HbR, respectively. The values of index *Q* were quantified as the area under the curve of the power amplitude of the FC time series across the low-frequency band (< 0.1Hz).

3.3 Differences in FC variability strength between different interregional connectivity

Figure 4(A) shows the connectivity groups with spatially different connectivity patterns (homotopic, long and short intrahemispheric and heterotopic connections). Generally, the long intrahemispheric connections showed a larger *Q* value than the other connections in both numerical (Fig. 4(B)) and statistical (Fig. 4(C)) analysis across HbO and HbR signals. In contrast, the index *Q* in homotopic and short intrahemispheric connections appeared to be numerically similar to each other, but smaller than that in the long intrahemispheric or heterotopic connections (Figs. 4(B) and 4(C)). The results indicate that, compared to the long intrahemispheric and heterotopic connections, the homotopic and short intrahemispheric connections maintain a less variable FC pattern during resting-state brain activity. Moreover, the analysis of static FC strength also produced the expected results. For example, the connectivity strength in long intrahemispheric connections was significantly smaller than that in homotopic and short intrahemispheric connections for both HbO and HbR signals. However, it is noteworthy that the difference of static connectivity strength between long intrahemispheric and heterotopic connections was not significant; whereas the index *Q* between the two groups was significantly different, irrespective of HbO or HbR signals. The results suggest that the FC fluctuation index, *Q*, relative to traditional static FC strength, is yet a more sensitive measure in distinguishing different interregional connectivity in the brain.

#237175 - $15.00 USD Received 30 Mar 2015; revised 27 May 2015; accepted 28 May 2015; published 5 Jun 2015

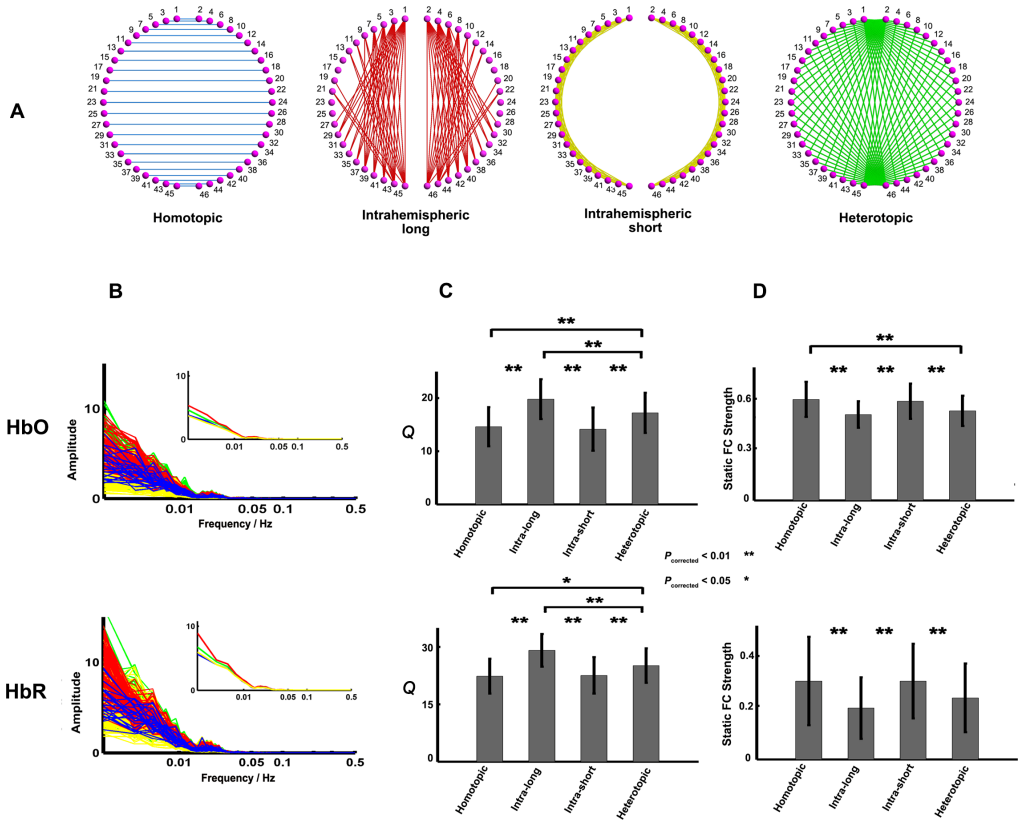

Fig. 4. *Q* difference and the static FC-strength difference in spatially different connectivity groups. (A) Configurations of selected connectivity groups (homotopic, long and short intrahemispheric and heterotopic connections) (B) Group-averaged power spectra of the dynamic FC time series in the four connectivity groups. The subplot showed the average of the power spectra across connections in each group. The lines with blue, red, yellow and green color represent the homotopic, long and short intrahemispheric and heterotopic connections, respectively. (C) Group differences in values of index *Q* between connectivity groups. (D) Group differences in static FC strength between connectivity groups. In (C and D), one and two asterisks represent significant group differences with permutation test at p <0.05 and 0.01 (Bonferroni-corrected), respectively. Error bars indicate standard deviations.

3.4 Validation

We evaluated the reproducibility of our primary findings in the study. First, using the current Session-1 data set, we separately changed the sliding-window sizes from 60 s to 30 s and 90 s to examine the impact of varying window lengths on dynamic FC findings. The main results, e.g., FC fluctuation *Q* was significantly negatively correlated with the static connectivity strength (Figs. 5(A) and 5(B)) and that the values of *Q* were significantly different between distinct interregional connectivity groups (Figs. 5(C) and 5(D)), kept good consistency compared to those obtained with 60-s sliding-window length (Figs. 3 and 4). This good reproducibility indicates that our findings were robust to different temporal window sizes. Meanwhile, we also noted that different window lengths led to different frequency spread patterns in respective power spectra of the FC time traces (Figs. 5(E) and 5(F)). Second, by using a separate fNIRS data set (Session 2), we also examined the reproducibility of our findings across scanning sessions. The fluctuation features in dynamic FC were kept consistent (Fig. 6) with the prior dynamic investigations using the Session-1 data set (Figs. 3 and 4).

#237175 - $15.00 USD Received 30 Mar 2015; revised 27 May 2015; accepted 28 May 2015; published 5 Jun 2015

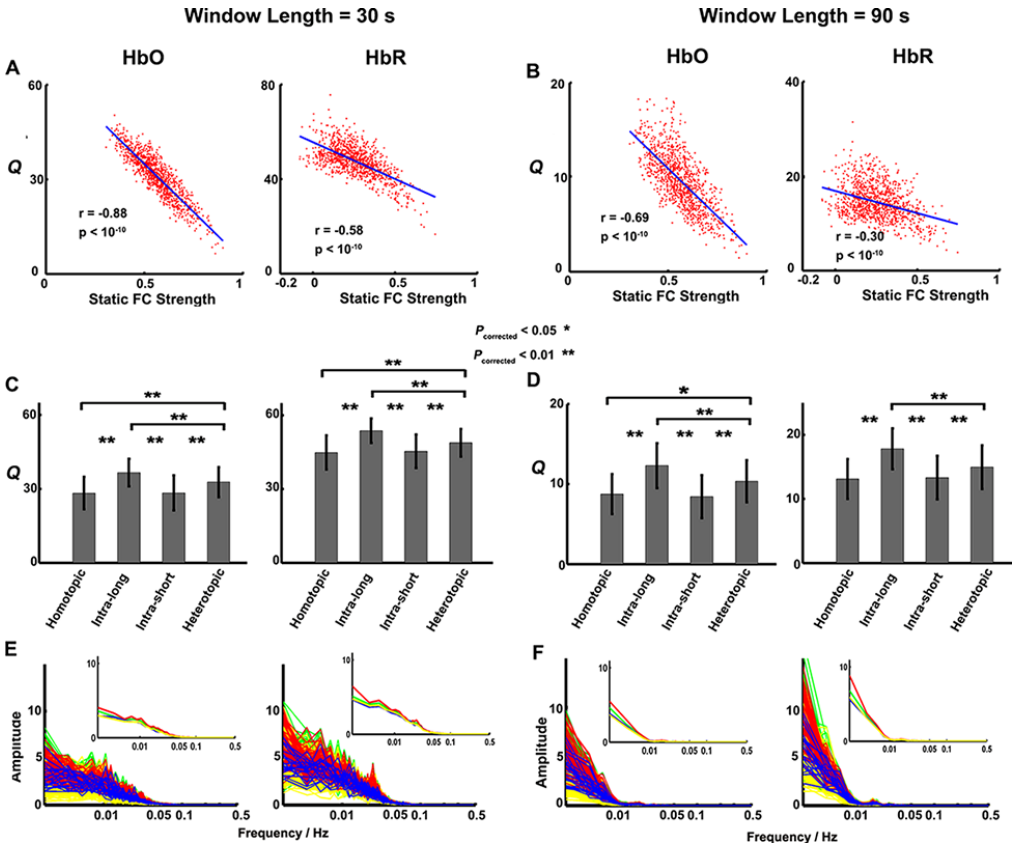

Fig. 5. Reproducibility of the primary findings derived from HbO and HbR signals over two various sliding-window lengths (30 s and 90 s). (A, B) The negative correlation relationship between index *Q* and the static connectivity strength. (C, D) The group differences in values of index *Q* between connectivity groups. (E, F). The group-averaged power spectra of dynamic FC time series in the four connectivity groups. The lines with blue, red, yellow and green color represent the homotopic, long and short intrahemispheric and heterotopic connections, respectively. All these results show good reproducibility over varying sliding-window lengths.

#237175 - $15.00 USD Received 30 Mar 2015; revised 27 May 2015; accepted 28 May 2015; published 5 Jun 2015

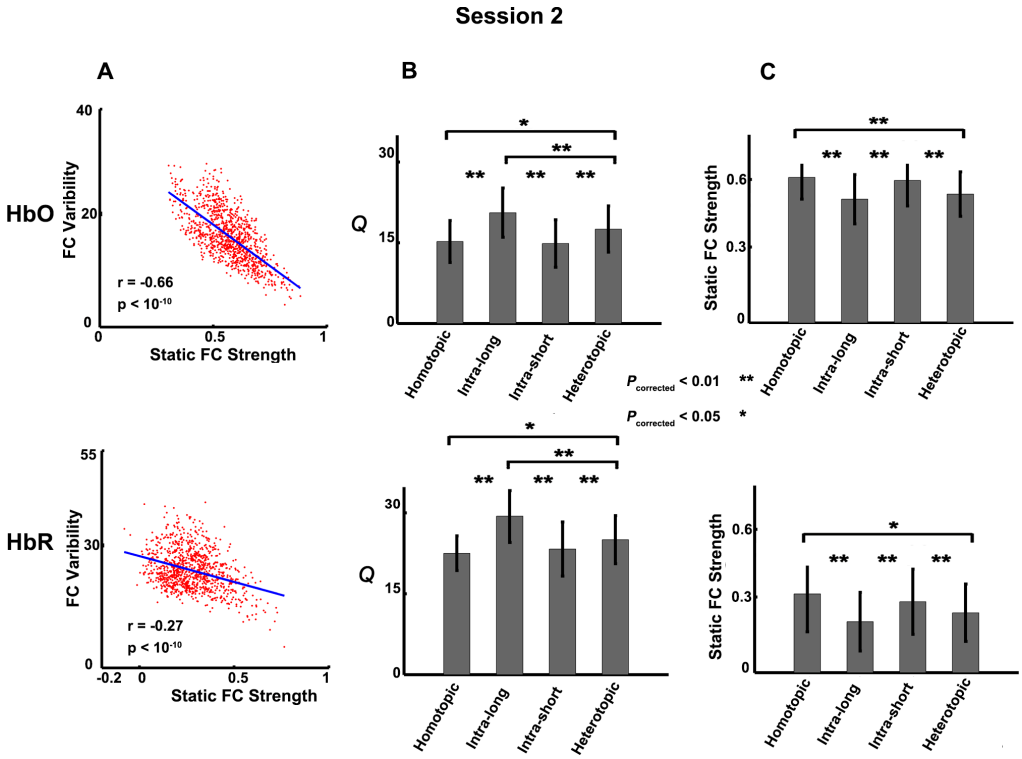

Fig. 6. Reproducibility of our primary findings derived from HbO and HbR signals across different fNIRS test data sets (Session 2). (A) The negative correlation relationship between index Q and static connectivity strength. (B, C) The group differences in values of index Q among four connectivity groups as well as the static connectivity strength among groups, respectively. The SWC approach with 60 s lengths was used to derive the dynamic FC.

4. Discussion

In this study, we explored the temporal characteristics of fNIRS-derived dynamic FC using SWC analysis. We found that the cortical FC network was highly variable over time (Fig. 2), and the variability strength Q in FC exhibited a significantly negative correlation relationship with the static FC strength (by the long-period fix-window analysis) (Fig. 3). Furthermore, the variability strength Q also showed significant differences between spatially various cortical locations/groups (i.e., homotopic, long and short intra-hemispheric and heterotopic connections), with a larger Q for long intrahemispheric connections and a smaller Q for homotopic and short intrahemispheric connections. The findings were highly reproducible, irrespective of sliding window lengths (Fig. 5) and recording sessions (Fig. 6), suggesting that the observed dynamic characteristics in the resting brain resulted from true cerebral fluctuation, rather than from non-cerebral physiological noise and/or movement artifacts. Collectively, our results derived from fNIRS signal correlations provide, to our knowledge, the first dynamic characterization of fNIRS-based FC and regional connectivity heterogeneity in FC variability in the range of whole-cortex regions. These results and their implications are discussed as follows.

The brain is a dynamic system even in the resting state. However, studies in the previous fNIRS-derived signal correlations merely characterized spatial features of the cerebral functional activity, and neglected temporal varying information included in it. Here, we introduced a dynamic analysis strategy (SWC) and for the first time investigated and explored temporal FC variations in the resting brain. Our results showed that the entire cortical FC was dynamic fluctuation over time (Fig. 2), consistent with previous investigations from other

#237175 - $15.00 USD Received 30 Mar 2015; revised 27 May 2015; accepted 28 May 2015; published 5 Jun 2015

neuroimaging techniques, such as EEG [4, 8], MEG [5], and fMRI [7], which indicated that the dynamic fluctuations in the brain FC represent a fundamental and essential property of normal brain function [33–36], whereas this property sustains the operation of the brain and its response to internal and external stimuli in a real time.

The results in Figs. 3(A) and 3(B) revealed that the organization of cortical networks with regard to increase or decrease in FC fluctuation strength depend on the cortical regions. For example, the index *Q* was found to be much bigger between the frontal and posterior cortical regions (Fig. 3(A)) in the entire cortical network. This observation was approximately in accordance with a previous dynamic study of resting-state fMRI that identified a group of more variable connections between brain regions of dorsal attention cortex, default-mode network, and superior occipital cortex [2]. Of note, the regions with great variable FC observed in our study and the previous fMRI study are of the most globally connected configuration in the whole-brain organization [37]. Meanwhile, some of the regions even consistently emerge as functional hubs in topological characterization of brain architecture [38], indicating heterogeneous and integrative functions of these great variable brain regions during dynamic brain activity. However, it needs to point out that the regions with more variable FC in cerebral cortex were generally neglected since the static FC strength between them were too small (Fig. 3(C)) to be significant. Herein, our current study based on all connections (i.e., including both strong and weak correlations) were expected to motivate FC analyses to focus on both weak and strong connections in the future study. Positive concerns on weak connections may bring about great benefit to identifying brain regions with more variable functional connections, which could be helpful in understanding roles of different functional systems in adaptive processes better.

Furthermore, in the present study, through categorizing the entire cortical FC into four distinct connectivity groups, we found that the values of index *Q* between connectivity groups had significant differences (Figs. 4 and 6), suggesting distinct physiological implication of FC fluctuation between different spatial locations of the brain system. Specifically, the long-range intrahemispheric connections, which mainly link brain regions of frontal and parietal/occipital regions, were consistently found to be more variable during resting-state brain activity across two scanning sessions (Figs. 4(C), 5(C) and 6(B)). The result also agreed well with one previous, task-derived fMRI study that demonstrated larger FC variability emerged in the regions between intrahemispheric frontal and postierior areas as experimental paradigm transformed from attention to memory-related tasks [39]. One of the possible underlying mechanisms leading to more variable in the long intrahemispheric connections in the brain organization is the less neural cooperation due to relatively less structural connections compared to others such as homotopic connections [40, 41]. Recently, it has also been pointed out that the more variable characteristics in long intrahemispheric connections potentially reflect a large-scale network with flexible capability in functional coordination between different neural systems [39]. For example, the frontal-posterior cortical regions are actively involved in high-level cognitive functions [42]; therefore, the larger variability in FC between these regions reflects quick processes to internal and external cognitive activity within the resting brain [39]. In contrast, the short range intrahemispheric and the symmetric homotopic connections are found to keep less variable during dynamic brain activity. One of the possible mechanisms underlying the observations may be the constraint of stronger structural connections during neural activities. Previous several studies using diffusion tensor imaging have indicated that different cortical regions whose hemodynamic fluctuations show strong correlation were connected directly through anatomical structures [43, 44]. Please also note that there exist brain regions that have no tract connections but show strong functional connection and relationship, such as medial prefrontal cortex and medial temporal lobes [43].

One of the important concerns in the dynamic FC study is whether the fluctuation in FC results from true cerebral fluctuation. Although the nature of FC variability during resting-state brain activity remains controversial [2, 7] and not yet fully understood, our present study

#237175 - $15.00 USD Received 30 Mar 2015; revised 27 May 2015; accepted 28 May 2015; published 5 Jun 2015

has shed light on this topic and has excluded the possibility of the FC fluctuation resulting from the influence of nonspecific physiological changes (e.g., cardiac or respiratory shifts) and/or head movement. Specifically, we conducted strict noise control during preprocessing procedures, such as adopting low frequency band-pass filtering and ICA denosing, which validly reduced the influence of typical noise components such as respiratory fluctuation (~0.2 Hz),cardiac pulsation (~1 Hz), motion-induced artifacts and skin blood flow fluctuation [26]. Certainly, we could not fully exclude the possibility that some portions of the low-frequency hemoglobin signals were contaminated by blood pressure and perfusion fluctuations from the extra-cranial tissue layers. However, our current two important findings, namely, (1) that FC variability Q has a significant and negative correlation with static FC strength (Fig. 3), and (2) that the values of index Q show significant differences between different interregional connectivity groups within the entire cortical regions (Fig. 4), could not be accounted for only by systemic noise sources and/or artifacts-contributions. More importantly, we excluded the contribution of systemic influences and/or artifacts by achieving a robust and reproducible result across two sessions of fNIRS recordings (Figs. 4 and 6). Thus, we conclude that the dynamic characteristics in fNIRS-derived hemodynamic signal correlations reflect the intrinsic properties of neural activity.

Several issues and further considerations need to be addressed. First, mapping the dynamic brain FC appropriately and precisely is a challenging task at the present stage of dynamic brain study [7]. We adopted a most commonly used approach, i.e., the SWC algorithm, to explore the dynamic brain FC characteristics; nevertheless, future studies employing other dynamic FC approaches, e.g., time-frequency coherence analysis with the wavelet transform, will possibly provide more detailed information and more comprehensive insights into the temporal variability properties of dynamic brain activity. Second, because the resting-state brain activity cannot completely exclude a subject's cognitive processes, it is also necessary to conduct task-evoked experiments to better explore and understand possible sources of low-frequency FC fluctuation. Meantime, approaches with multimodal imaging, such as simultaneous measurements of fNIRS with EEG or with electrophysiology recording, may also provide us with a vital chance to reveal a potential mechanism for information processing in the brain such as information exchange between different brain states. Third, one notable advantage of the fNIRS tool is its capability for long-period data acquisition because of less physical burden and body confinement on participants. This feature will allow researchers to record state transitions in each individual participant and obtain their repeated connectivity patterns in the brain, which may be critical for future dynamic studies that examine relationships between FC fluctuation and behavioral variability within and between participants. Finally, we also need to note a few limitations of our fNIRS-derived dynamic FC study. Since low penetration depth is a known drawback of fNIRS brain imaging, it limits researchers to investigate intrinsic FC and/or its fluctuations only from cortical regions in large scales of functional systems (e.g., motor or visual regions). Even for small-sized animal studies, such as rats or mice, another drawback of fNIRS is its low spatial resolution. In comparison, a new technology based on photoacoustic resting-state FC imaging (fcPAT), which utilizes optical excitation and acoustic detection, allows studies of functional brain network with a high spatial resolution in small animals [45]. Therefore, it is expected that the employment of fcPAT in small animals may provide rich information on dynamic resting-state FC network and hence advance the understanding of how dynamic network properties support normal brain functions.

Overall, this study has demonstrated the feasibility of using whole-cortical fNIRS time series to derive dynamic FC in the human brain. While the static method calculates a relatively slow temporal correlation and provides a convenient framework to examine rather stable functional brain circuits and remote network connections, dynamic resting-state FC offers a tool for researchers to gain insight into the relationship between time-varying macroscopic neural activity patterns and critical aspects of cognition and behavior. Overall,

#237175 - $15.00 USD Received 30 Mar 2015; revised 27 May 2015; accepted 28 May 2015; published 5 Jun 2015

studies on both static and dynamic brain FC network are complementary and warrant equal attention in future research.

Appendix

Table 1. Correlation coefficient, *r*, between *Q* and static FC strength at the individual level

Subject	HbO		HbR	
	r	***p***	***r***	***p***
1	–0.91	$<10^{-10}$	–0.64	$<10^{-10}$
2	–0.76	$<10^{-10}$	–0.03	$<10^{-10}$
3	–0.77	$<10^{-10}$	–0.05	0.02
4	–0.85	$<10^{-10}$	–0.47	$<10^{-10}$
5	–0.59	$<10^{-10}$	–0.47	$<10^{-10}$
6	–0.79	$<10^{-10}$	–0.49	$<10^{-10}$
7	–0.87	$<10^{-10}$	–0.63	$<10^{-10}$
8	–0.72	$<10^{-10}$	–0.20	$<10^{-9}$
9	–0.78	$<10^{-10}$	–0.57	$<10^{-10}$
10	–0.85	$<10^{-10}$	–0.31	$<10^{-10}$
11	–0.81	$<10^{-10}$	–0.55	$<10^{-10}$
12	–0.66	$<10^{-10}$	–0.07	0.02
13	–0.81	$<10^{-10}$	–0.75	$<10^{-10}$
14	–0.72	$<10^{-10}$	–0.35	$<10^{-10}$
15	–0.70	$<10^{-10}$	–0.22	$<10^{-10}$
16	–0.51	$<10^{-10}$	–0.22	$<10^{-10}$
17	–0.20	$<10^{-10}$	–0.01	0.77
18	–0.74	$<10^{-10}$	–0.20	$<10^{-10}$
mean	–0.72		–0.35	
std	0.16		0.23	

(Note: Individual values of *Q* and static FC strength for each subject are not listed here but used to quantify *r* and *p*, where *p* represents the statistical parameter used to compare with the significance level of a statistical hypothesis test.)

#237175 - $15.00 USD Received 30 Mar 2015; revised 27 May 2015; accepted 28 May 2015; published 5 Jun 2015

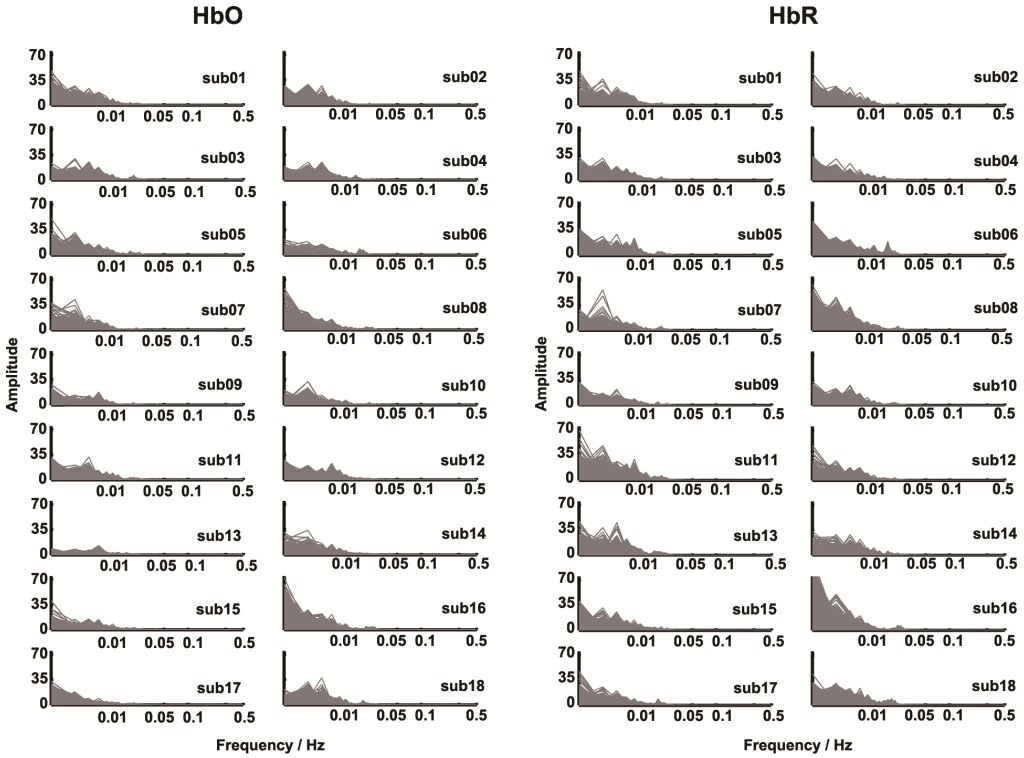

Fig. 7. Power spectral analyses of dynamic FC time series for all 18 subjects and two types of hemoglobin concentration signals (HbO and HbR). The sliding-window length was 60 s. In each panel, there are 46 × 45/2 power spectra curves that are overlapped and become a gray-shaded area.

Acknowledgments

This study is supported by the Natural Science Foundation of China (Grant Nos. 81201122 and 81030028), the National Science Fund for Distinguished Young Scholars (Grant No. 81225012), the Fundamental Research Funds for the Central Universities (Grant No. 2012LYB06), the Specialized Research Fund for the Doctoral Program of Higher Education, and the Open Research Fund of the State Key Laboratory of Cognitive Neuroscience and Learning.

#237175 - $15.00 USD Received 30 Mar 2015; revised 27 May 2015; accepted 28 May 2015; published 5 Jun 2015